# BOLD Signal and Task-Correlated Respiratory Events

**Sam Zorowitz**

**Abstract** We investigate the effects of task-correlated respiratory events on the detection and estimation of fMRI BOLD signal. Through experiments involving visual stimulation, breath-holding, and hyperventilation, we find task-correlated respiratory events result in extensive detection of false-positive activations and reduced ability to estimate true BOLD signal change in visual cortex. We also find that the CompCor respiration nuisance regressors are only partially able to improve detection and estimation power. Recommendations for future research are discussed.

## Introduction

The goal of functional magnetic resonance imaging (fMRI) is to measure variation in the blood oxygenation level dependent (BOLD) signal as a proxy for changes in neural activity. This goal is stymied by the fact that the signals of interest are often much smaller in magnitude than noise from both the scanner and participant (Huettel et al., 2004; Caballero-Gaudes and Reynolds, 2017).

Participant respiration is one source of noise caused by changes in arterial levels of carbon dioxide. Respiratory events can be categorized as either hypercapnic (i.e. an increase in arterial $CO_2$) or hypocapnic (i.e. a decrease in arterial $CO_2$). Previous research has shown that induced hypercapnic events (e.g. breath-holding) results in substantial increases in the whole-brain BOLD signal (Kastrup et al., 1999a, 1999b), whereas induced hypocapnic events (e.g. hyperventilation) results in substantial decreases (Bright et al., 2009). Even small, naturally-occurring changes in breathing patterns yield measurable deflections of the BOLD signal (Van den Aardweg and Karemaker, 2002; Wise et al., 2004; Birn et al., 2006; Bianciardi et al., 2009a, 2009b). Despite this, previous studies have found that respiratory (and related cardiac signals) account for less than 10% of the BOLD noise on average over the whole brain (Shmueli et al., 2007; Bianciardi et al., 2009a, 2009b). As such, most task-based fMRI studies ignore respiratory noise during analysis.

More recently, rhe neuroimaging community has shown renewed interest in controlling for respiratory noise in task-based fMRI analysis. One reason for this is growing recognition of task-correlated changes in breathing rate, wherein changes in respiratory events are time-locked to an experimental event of interest (Napadow et al., 2008; Birn et al., 2009; Huijbers et al., 2014). If unaccounted for, task-correlated respiration can yield result in finding spurious effects and/or mask true effects (Birn et al., 2009). A second reason is recent research which found that a substantial proportion of head motion can be explained by transient respiratory events (e.g. sudden inhale/exhale; Power et al., 2018). This has prompted calls for new research to better understand and de-noise respiration artifact for task-based fMRI data (Kundu et al., 2013; Power et al., 2018).

Here, we highlight the effects of induced respiratory events on measured BOLD signal. Specifically we demonstrate the effects of hypercapnic and hypocapnic events, resulting from periods of instructed breath-holding and hyperventilation, on measuring BOLD signal during a visual stimulation paradigm. We find that task-correlated changes in respiration result in a considerable increase in false-positive activations and also reduce detection of true activation. We also show that commonly-used nuisance regressors, CompCor (Behzadi et al., 2007), can improve task-based BOLD analysis (albeit imperfectly).

## Results

The effects of task-correlated respiratory artifact was measured in two participants. Participants each completed five runs of functional scanning. In the first run, participants viewed, flashing, rotating visual checkerboards (condition: **VZ**). Next, participants

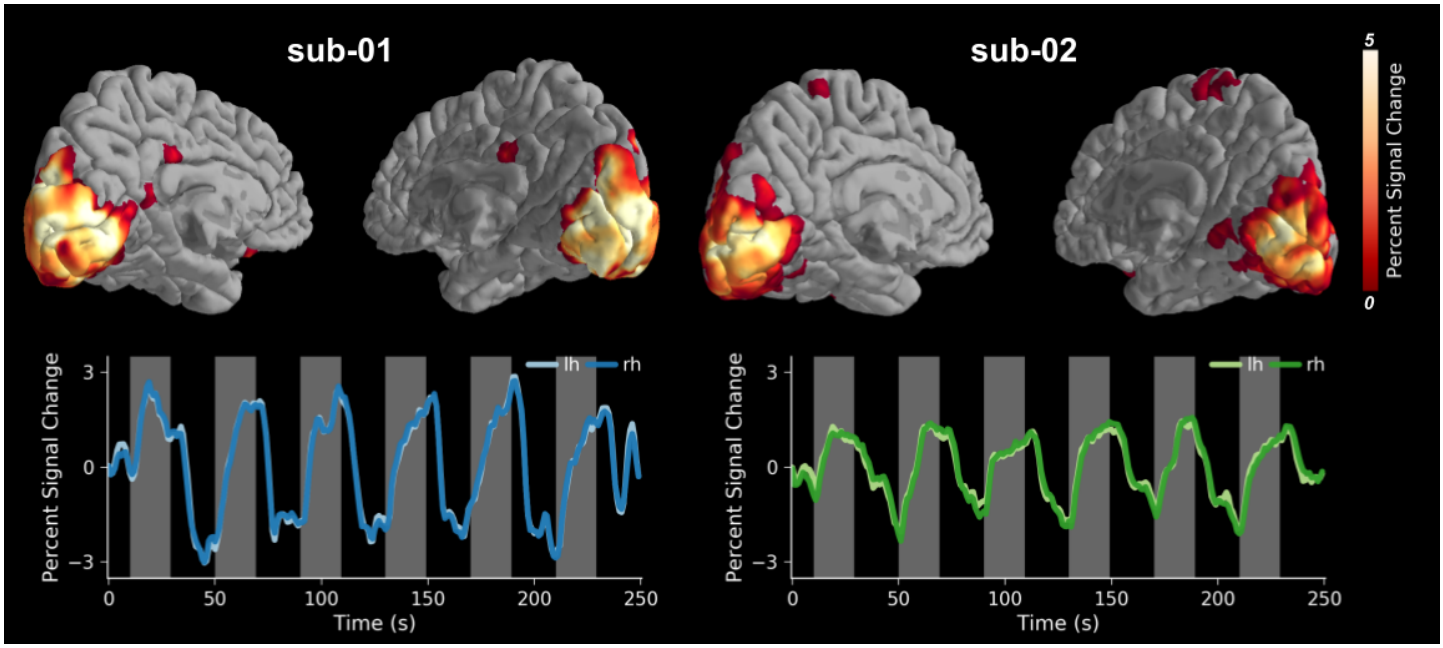


**Figure 1. Activation maps for visual stimulation**
Significant voxel-wise increases in BOLD signal (top) in response to the checkerboard stimuli were selective to the visual cortex. Passive viewing of the stimuli elicited BOLD signal changes of approximately 2-3% across participants (bottom).

---

viewed the same stimuli while either holding their breath (condition: **V-BH**) or hyperventilating (condition: **V-HV**). For each run, the cortical response to the visual stimulus was estimated via regression with an idealized stimulus function (see Methods for complete details). The fourth and fifth runs measured the change in BOLD signal to breath-holding (condition: **BH**) and hyperventilation (condition: **HV**) in isolation.

### Checkerboard stimuli selectively activate visual cortex

To understand the impact of respiration on measured BOLD signal, we must first establish a baseline must first be established. In visual stimulation condition (**VZ**), participants viewed six visual checkerboard stimuli in blocks of 20s. We then regressed an idealized stimulus response against the BOLD timeseries measured at each voxel separately for each participant. Visual stimulation using the checkerboard stimuli yielded robust bilateral activation in visual cortex for both participants (Figure 1). Separate anatomical masks were generated from the significantly active voxels within each hemisphere. The average BOLD signal timeseries for voxels within these masks are also presented in Figure 1. For the first participant, the significantly active voxels of the left and right hemispheres showed a signal increase of 3.11% (se = 0.33%) and 3.13% (se = 0.35%), respectively. For the second participant, significantly active voxels of the left and right hemispheres showed a signal increase of 1.67% (se = 0.27%) and 1.70% (se = 0.23%), respectively. In sum, the checkerboard stimuli were successful in evoking robust BOLD signal change in the visual cortex of both participants.

### Task-correlated respiratory events severely disrupt BOLD signal measurement

Before turning to their disruptive effects, we first measure the stereotyped BOLD signal change in response to respiratory events. In the breath-holding (**BH**) and hyperventilation (**HV**) conditions, participants were instructed to hold their breaths and hyperventilate for six blocks of 20s. The averaged cortical BOLD change aligned to the onset breath-holding/hyperventilating are presented in Figure 2. Consistent with prior studies of hypercapnic events, breath-holding resulted in an initial reduction in BOLD signal followed by a prolonged period of BOLD signal increase peaking around 25-30s (Kastrup et al., 1999a, 1999b; Birn et al., 2009; Bright et al., 2009). By contrast, hyperventilation resulted in the opposite pattern: an initial increase in BOLD signal followed by a prolonged period of BOLD signal decrease peaking around 30s. Again this is consistent with previous research (Bright et al., 2009). In sum, the change in cortical BOLD signal in response to breath-holding and hyperventilation was consistent across participants and opposite in effect: breath-holding yields a sustained increase in BOLD signal, whereas hyperventilation yields a sustained decrease.

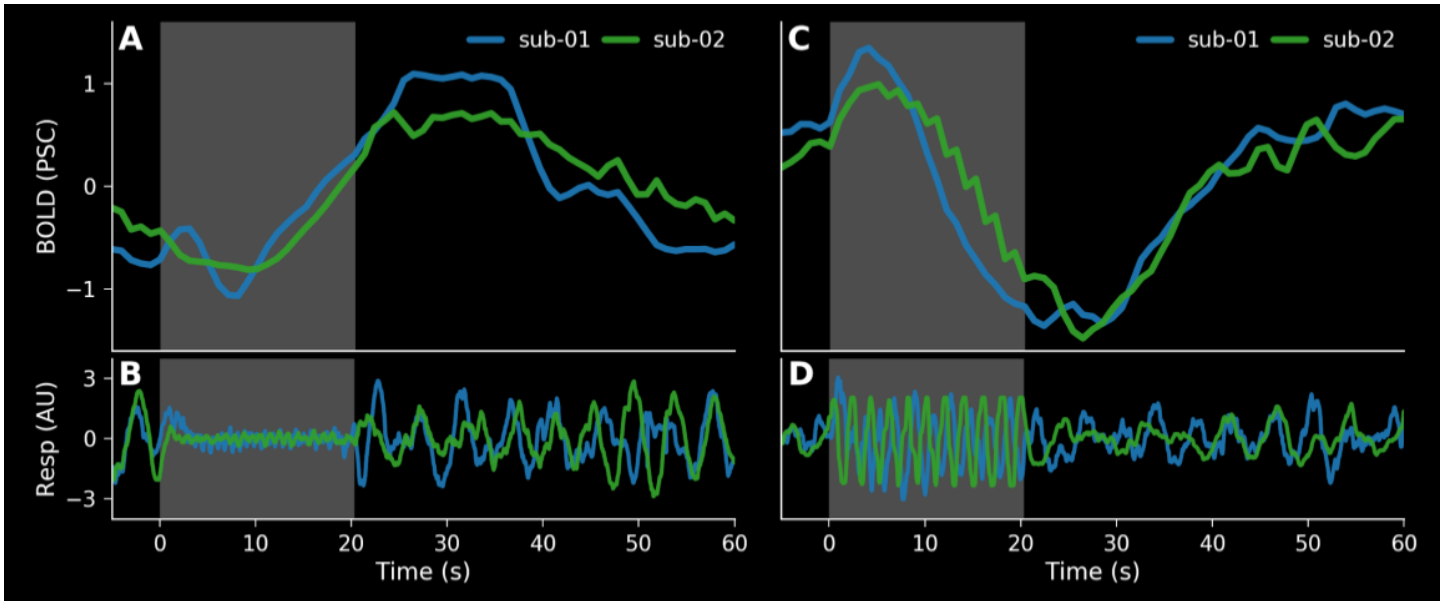


**Figure 2. Effects of respiratory events on BOLD**
The time-locked responses of BOLD signal to breath-holding (A) and hyperventilation (C) show consistent, opposite patterns. Periods of breath-holding and hyperventilation signified by shaded regions, as evidenced by the physiological respiratory traces (B,D).

---

Interestingly, the effects of task-correlated respiratory events are heterogeneous across both participants and cortical anatomy. For example, diffuse false-positive activation was detected across the frontal lobe of participant 1 during breath-holding, where comparably more sparse false-positive activation was detected for participant 2. Similarly, false-positive deactivation was detected diffusely across the temporal and parietal lobes of participant 2 during hyperventilation, whereas false-positive deactivation was primarily located in the frontal lobe for participant 1. This suggests individual differences in the vasculature between participants, consistent with previous findings (Bright et al., 2009).

Next, we investigate the effects of task-correlated respiratory events on fMRI detection power. In the visual breath-holding (**V-BH**) and visual hyperventilation (**V-HV**) conditions, participants were again instructed to hold their breaths and hyperventilate for six blocks of 20s while viewing the same checkerboard stimuli. We again regressed an idealized stimulus response to the checkerboard stimuli against the BOLD timeseries measured at each voxel without including any additional regressors controlling for the respiratory events. As compared to the visual-only condition (**VZ**), significant activation was detected across the entire cortex of both participants (Figure 3). As would be expected, positive activation (i.e. increase in BOLD signal) was detected across the cortex in the **V-BH** condition whereas negative activation (i.e. decrease in BOLD signal) was detected across the cortex. Insofar that the checkerboard stimuli should only activate visual cortex (Figure 1), these widespread significant activations are false-positives (i.e. non-neural in origin) and represent a substantial decrease in the statistical power to detect neural-in-origin changes in BOLD signal.

Next, we investigate the effects of task-correlated respiratory events on measured BOLD signal change estimation. Using the masks of visual cortex defined above, we compared the percent signal change of the checkerboard stimulus response regressor between conditions, averaging across the hemispheres within participants. The results of all the pairwise contrasts are reported in Table 1. In the first participant, a significant reduction in percent signal change of visual cortex BOLD was observed between VZ and V-HV ($F = 38.19$, $p < 0.001$) but not between VZ and V-BH ($F = 0.04$, $p = 0.848$). In the second participant, a significant reduction in the percent signal change of visual cortex BOLD was observed between VZ and V-BH ($F = 24.45$, $p < 0.001$) and VZ and V-HV ($F = 20.94$, $p < 0.001$).

In summary, we found that task-correlated respiratory artifact is profoundly detrimental to task-based fMRI analysis when uncontrolled for. Breath-holding and hyperventilation contemporaneous with visual stimulation both resulted in detection of extensive false-positive activations, as well as impeded the ability to measure true BOLD change. Thus, task-correlated respiratory diminishes both fMRI detection and estimation power.

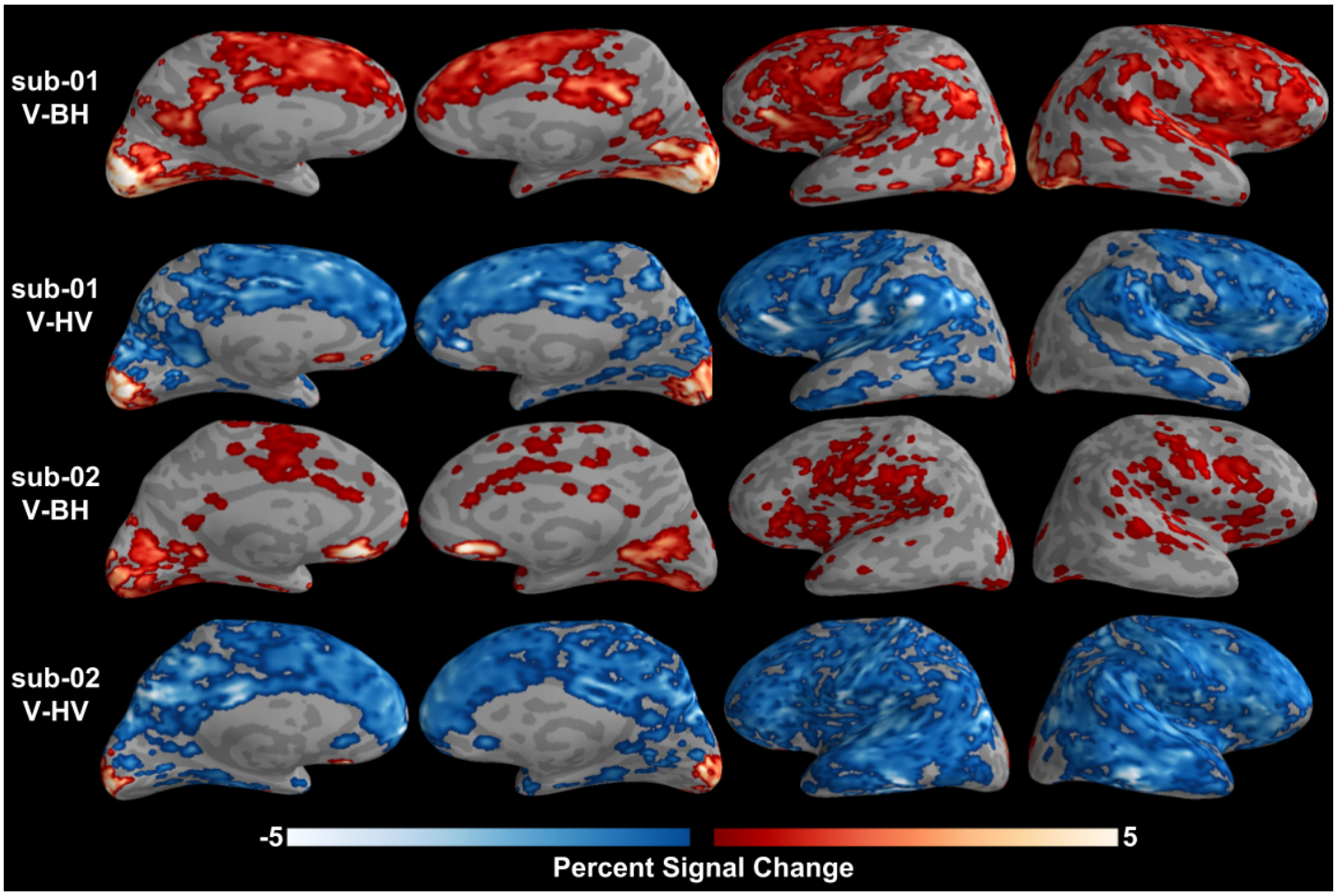


**Figure 3. Activation maps for visual breath-holding and visual hyperventilation**
Widespread false-positive activations and deactivations were detected in response to visual stimuli while breath-holding (V-BH) or hyperventilation (V-HV). Participants exhibit notable heterogeneity in activation extents across tasks and cortical regions.

| Subject | Analysis | L PSC | R PSC | F-val | p-val |
|---|---|---|---|---|---|
| | VZ | 3.11 (0.33) | 3.13 (0.35) | | |
| | V-BH | 3.13 (0.38) | 2.98 (0.36) | 0.04 | 0.848 |
| 01 | V-BH + CompCor | 2.33 (0.20) | 2.25 (0.20) | 13.42 | <0.001 |
| | V-HV | 1.53 (0.17) | 1.41 (0.16) | 38.19 | <0.001 |
| | V-HV + CompCor | 2.28 (0.18) | 2.16 (0.17) | 17.29 | <0.001 |
| | VZ | 1.67 (0.27) | 1.70 (0.23) | | |
| | V-BH | 0.54 (0.23) | 0.41 (0.24) | 24.45 | <0.001 |
| 02 | V-BH + CompCor | 0.30 (0.14) | 0.18 (0.14) | 73.14 | <0.001 |
| | V-HV | 0.44 (0.14) | 1.05 (0.14) | 20.94 | <0.001 |
| | V-HV + CompCor | 0.97 (0.13) | 1.59 (0.13) | 5.80 | 0.016 |

**Table 1. Percent Signal Change in Visual Cortex**

Summary of visual cortex BOLD signal change in response to visual stimulation. Reported are percent signal change estimates with standard errors across participants (01, 02), hemispheres (left = L, right = R), conditions (visual stimuli only = VZ; visual breath-holding = V-BH; visual hyperventilation = V-HV), and inclusion of respiratory nuisance regressors. Within-subjects pairwise contrasts were estimated, averaging across hemispheres, to test for significant differences in signal change as compared to control (VZ).

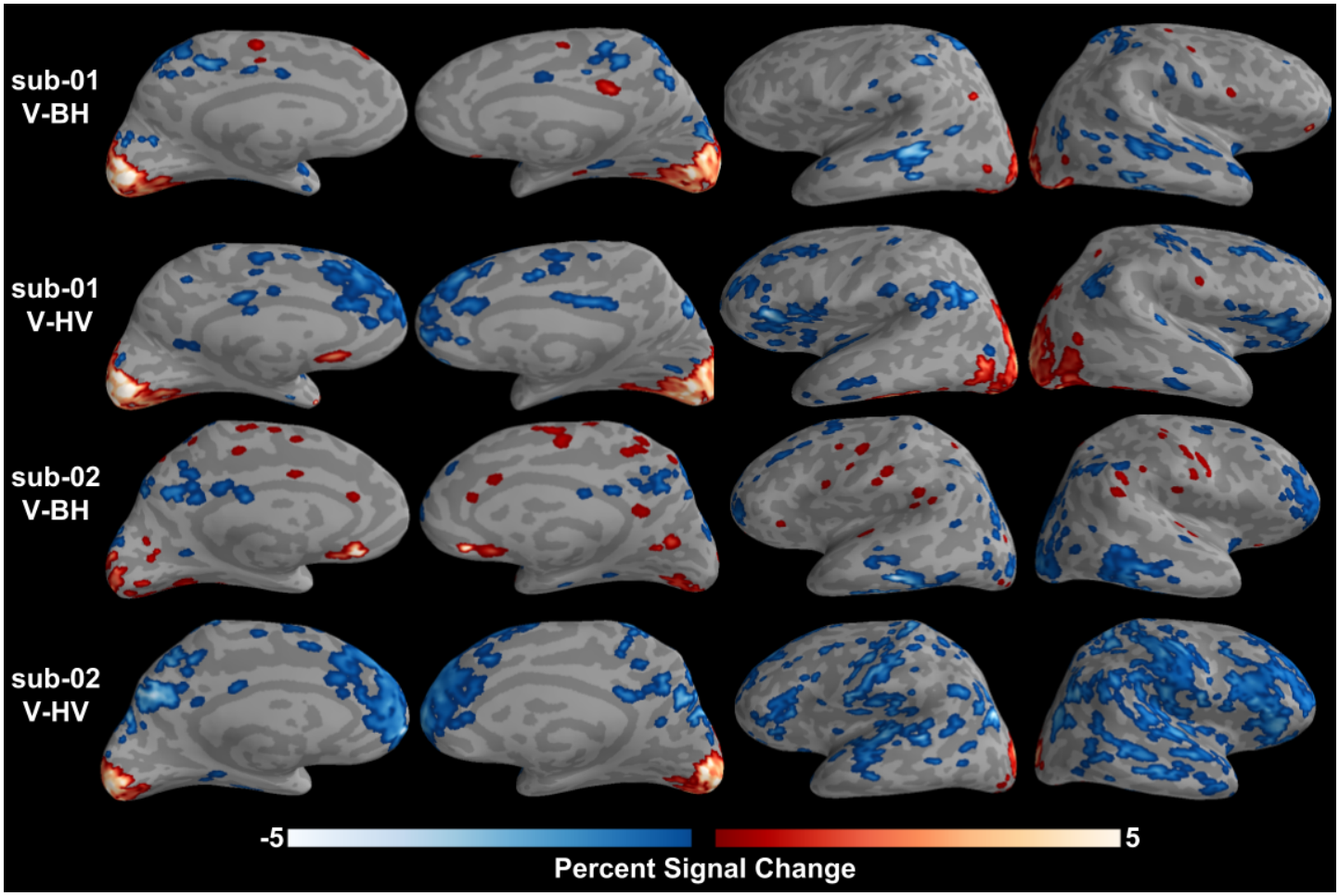


**Figure 4. Correcting for artifact with CompCor**

## CompCor improves the detection and estimation of BOLD signal

To control for the effects of task-correlated respiratory events, we then re-estimated the regression models for the V-BH and V-HV conditions now including the CompCor regressors (Behzadi et al., 2007). Briefly, CompCor (i.e. *Component Based Noise Correction*) estimates nuisance regressors from the principal components of the BOLD timeseries of the cerebrospinal fluid (CSF) and white matter (WM), where neural activity is unlikely to be contributing to BOLD signal. The inclusion of CompCor regressors when estimating the change in BOLD in response to the visual stimuli substantially reduces the number of false-positive activations (Figure 4). Importantly CompCor does not completely reduce false-positive activations. Interestingly, the false-positive activations detected when including CompCor seem to be predominantly negative. The reasons for this are unclear, but may have to do with anatomical differences in the vasculature across the brain.

With regards to CompCor and estimation power, we find similarly mixed results (Table 1). In both participants, the inclusion of CompCor was found to improve recovery of the true BOLD signal during hyperventilation (i.e. percent signal change in visual cortex is increased when including CompCor), though the estimates were still significantly reduced as compared to control (participant 1: $F = 17.29$; $p < 0.001$; participant 2: $F = 5.80$, $p = 0.016$). By contrast, the inclusion of CompCor was found to decrease recovered estimates of the BOLD signal change in visual cortex during breath-holding (Table 1). As such, it appears that CompCor may be beneficial in improving fMRI detection and estimation power. The present results highlight, however, the need for careful paradigm design and participant coaching in preventing task-correlated respiratory artifact in the first place.

Finally, for the sake of completeness, we note we attempted to construct a custom respiration nuisance regressor based on the stereotyped BOLD responses to breath-holding and hyperventilation. We found the resulting regressors were highly collinear with the checkerboard stimulus regressor and thus prohibitive for calculating an approximate inverse in regression.

## Discussion

In this brief experiment, we investigated the effects of task-correlated respiratory events on the detection and estimation of fMRI BOLD signal. We found that breath-holding and hyperventilation contemporaneous with visual stimulation resulted in extensive detection of false-positive activations and reduced ability to estimate true BOLD signal change in visual cortex. The CompCor respiration nuisance regressors were only partially able to reduce false positives and recover BOLD activation. The present results demonstrate the importance of controlling for and, more importantly, preventing task-correlated respiratory artifact. Future studies should investigate novel methods for controlling for respiration artifact and techniques for coaching participants on non-disruptive breathing.

## Methods

### Participants

Two participants (both female, age 25) volunteered to participate in this experiment as part of a course on cognitive neuroscience methods. Both participants reported being right-handed and without a current or past diagnosis of a psychiatric or neurological disorder. All experimental procedures were approved by the NEU502b course instructors.

### Task Paradigms

**Visual Stimulation** The visual stimulation task was used to localize BOLD signal change in the visual cortex of participants. Participants viewed a rotating, flashing black-and-white checkerboard stimulus. The stimuli were presented in six 20s blocks with 20s of fixation cross in-between. The run lasted 250s and was completed once per participant.

**Breath-holding** The breath-holding task was used to measure the physiological BOLD response to a hypercapniac event. Participants were instructed to hold their breath for six blocks of 20s. Each block was followed by a recovery period of 40s. The run lasted 370s and was completed once per participant. The task was designed based on previous research (Birn et al., 2009).

**Hyperventilate** The hyperventilation task was used to measure the physiological BOLD response to a hypocapniac event. Participants were instructed to rapidly inhale then exhale with each action lasting 2s. Participants hyperventilated for six blocks of 20s. Each block was followed by a recovery period of 40s. The run lasted 370s and was completed once per participant. The task was designed based on previous research (Bright et al., 2009).

**Visual Breath-holding** The visual breath-holding task was designed to measure the effects of a hypercapniac event on BOLD detection during visual stimulation. Participants were instructed to hold their breath for six blocks of 20s. 10s into each each block, the checkerboard stimulus as above was presented for 20s. In other words, the breath-holding and visual stimulation blocks each lasted 20s and were staggered by 10s. Each block was followed by a recovery period of 30s. he run lasted 370s and was completed once per participant.

**Visual Hyperventilation** The visual hyperventilation task was designed to measure the effects of a hypocapnic event on BOLD detection during visual stimulation. Participants were instructed to hyperventilate as above for six blocks of 20s. 10s into each each block, the checkerboard stimulus as above was presented for 20s. In other words, the hyperventilation and visual stimulation blocks each lasted 20s and were staggered by 10s. Each block was followed by a recovery period of 30s. he run lasted 370s and was completed once per participant.

The visual stimuli were programmed in Python and Psychopy (Peirce, 2008), and were presented with a projector. Participants viewed the projection on a screen fixed at the back of the scanner bore, through a mirror fixed in front of the eyes.

### Data Acquisition

Briefly, all images were acquired with a 64 channel head coil on a 3T Siemens Prisma. A T1-weighted MPRAGE image was acquired with TR=2530 ms, TE 3.31 ms, flip angle=7 deg, in-plane FOV=256 x 256 mm, 176 slices, 1.0 mm isotropic voxels. For advanced anatomical registration (see below), a T2-weighted image was acquired TR=3200 ms, TE=428 ms, flip angle=120 deg, in-plane FOV=256 × 256 mm, 72 slices, 1.0 mm isotropic voxels. Whole-brain EPI acquisitions were acquired with TR=1000 ms, TE=30 ms, flip angle=55 deg, in-plane FOV=192 × 192 mm, 56 slices, 3.0 mm isotropic voxels, with a multi-band acceleration factor of 4. One

run of each task was acquired with anterior-to-posterior phase encoding. Prior to the collection of the EPI images, a fieldmap was acquired for the purposes of susceptibility distortion correction (see below) with TR=1000 ms, TE=3.47 ms, flip angle=120 deg, in-plane FOV=192 × 192 mm, 56 slices, 3.0 mm isotropic voxels.

To measure cardiac and respiratory signals, a pulse oximeter and respiratory bellows were fitted to participants prior to the scanning. The pulse and respiratory signals were recorded by the scanner host computer at a sampling rate of 200 Hz and 50 Hz, respectively. The recordings were aligned with the onset of the first sync pulse using a custom script.

## Data Preprocessing

Results included in this manuscript come from preprocessing performed using FMRIPREP v1.0.8 (Esteban et al., 2018), a Nipype based tool (Gorgolewski et al., 2011, 2017). Each T1w (T1-weighted) volume was corrected for INU (intensity non-uniformity) using *N4BiasFieldCorrection* v2.1.0 (Tustison et al., 2010) and skull-stripped using *antsBrainExtraction.sh* v2.1.0 (using the OASIS template). Brain surfaces were reconstructed using *recon-all* from FreeSurfer v6.0.0 (Dale et al., 1999), and the brain mask estimated previously was refined with a custom variation of the method to reconcile ANTs-derived and FreeSurfer-derived segmentations of the cortical gray-matter of Mindboggle (Klein et al., 2017). Spatial normalization to the ICBM 152 Nonlinear Asymmetrical template version 2009c (Fonov et al., 2009) was performed through nonlinear registration with the *antsRegistration* tool of ANTs v2.1.0 (Avants et al., 2008), using brain-extracted versions of both T1w volume and template. Brain tissue segmentation of cerebrospinal fluid (CSF), white-matter (WM) and gray-matter (GM) was performed on the brain-extracted T1w using *fast* (FSL v5.0.9) (Zhang et al., 2001).

Functional data was motion corrected using *mcflirt* (FSL v5.0.9; Jenkinson et al., 2002). Slice timing was not performed in light of the task design and short repetition time. Distortion correction was performed using an implementation of the TOPUP technique (Andersson et al., 2003) using *3dQwarp* (AFNI v16.2.07; Cox, 1996). This was followed by co-registration to the corresponding T1w using boundary-based registration (Greve and Fischl, 2009) with 9 degrees of freedom, using *bbregister* (FreeSurfer v6.0.0). Motion correcting transformations, field distortion correcting warp, BOLD-to-T1w transformation and T1w-to-template (MNI) warp were concatenated and applied in a single step using *antsApplyTransforms* (ANTs v2.1.0) using Lanczos interpolation.

Physiological noise regressors were extracted applying CompCor (Behzadi et al., 2007). Principal components were estimated for the two CompCor variants: temporal (tCompCor) and anatomical (aCompCor). A mask to exclude signal with cortical origin was obtained by eroding the brain mask, ensuring it only contained subcortical structures. Six tCompCor components were then calculated including only the top 5% variable voxels within that subcortical mask. For aCompCor, six components were calculated within the intersection of the subcortical mask and the union of CSF and WM masks calculated in T1w space, after their projection to the native space of each functional run. Framewise displacement (Power et al., 2014) was calculated for each functional run using the implementation of Nipype.

Many internal operations of FMRIPREP use *Nilearn* (Abraham et al., 2014), principally within the BOLD-processing workflow. For more details of the pipeline see https://fmriprep.readthedocs.io/en/latest/workflows.html.

Image quality was assessed using MRIQC v0.10.4 (Esteban et al., 2017). Both anatomical and functional scans were visually inspected for artifacts and showed no apparent defects. The QC reports, including carpet plots of the raw BOLD signal (Power, 2017), are included for reviewer inspection.

## Data Analysis

Prior to analysis, all functional data were downsampled from the native Freesurfer brain meshes ( 140,000 vertices per hemisphere) to the *fsaverage5* template brain (10242 vertices per hemisphere). This downsamplign procedure is approximately equivalent to applying spatial smoothing with FWHM of approximately 6 $mm^2$. To remove low frequency drift terms, functional data were high-passed filtered at 100s using Nilearn.

Activation maps in response to the visual checkerboard stimuli were estimated by for the visual stimulation, visual breath-holding, and visual hyperventilation tasks by regressing the BOLD timeseries at each voxel against an idealized stimulus response function. Here, the stimulus response function was computed by convolving a boxcar function (corresponding to the onset/offset times of the visual checkerboard stimuli) with the canonical hemodynamic response function.

For all regression analyses, motion regressors and scrubbers were included. The motion regressors were comprised of the timeseries of the six degrees of motion after being de-meaned, linearly detrended, and orthogonalized with principal components analysis. Motion scrubbers were used to regress our the effects of volumes with high motion artifact, here defined as framewise displacement (FD) > 0.5 mm as previously recommended (Power et al., 2014; Siegel et al., 2014). The motion scrubbers consist of a column of zeros except for a 1 in the row corresponding to the motion-contaminated volume. Across all runs, only 3 volumes exhibited FD > 0.5 mm. In the final regression analyses controlling for respiration artifact, the anatomical CompCor regressors estimated by FMRIPREP were used.

To correct for temporal autocorrelation, the data and design matrices were prewhitened using a Tukey taper approach (Woolrich et al., 2001). Multiple comparisons corrections across voxels were implemented via permutation testing with 5000 null permutations and family-wise error correction at alpha = 0.05 (Winkler et al., 2014). The resulting activation maps were projected back onto the native freesurfer brains for visualization.

## References


**Van den Aardweg JG**, Karemaker JM. Influence of chemoreflexes on respiratory variability in healthy subjects. Am J Respir Crit Care Med. 2002 Apr; 165(8):1041–1047.

**Abraham A**, Pedregosa F, Eickenberg M, Gervais P, Mueller A, Kossaifi J, Gramfort A, Thirion B, Varoquaux G. Machine learning for neuroimaging with scikit-learn. Front Neuroinform. 2014 Feb; 8:14.

**Andersson JLR**, Skare S, Ashburner J. How to correct susceptibility distortions in spin-echo echo-planar images: application to diffusion tensor imaging. Neuroimage. 2003 Oct; 20(2):870–888.

**Avants BB**, Epstein CL, Grossman M, Gee JC. Symmetric diffeomorphic image registration with cross-correlation: evaluating automated labeling of elderly and neurodegenerative brain. Med Image Anal. 2008 Feb; 12(1):26–41.

**Behzadi Y**, Restom K, Liau J, Liu TT. A component based noise correction method (CompCor) for BOLD and perfusion based fMRI. Neuroimage. 2007 Aug; 37(1):90–101.

**Bianciardi M**, Fukunaga M, van Gelderen P, Horovitz SG, de Zwart JA, Duyn JH. Modulation of spontaneous fMRI activity in human visual cortex by behavioral state. Neuroimage. 2009 Mar; 45(1):160–168.

**Bianciardi M**, Fukunaga M, van Gelderen P, Horovitz SG, de Zwart JA, Shmueli K, Duyn JH. Sources of functional magnetic resonance imaging signal fluctuations in the human brain at rest: a 7 T study. Magn Reson Imaging. 2009 Oct; 27(8):1019–1029.

**Birn RM**, Diamond JB, Smith MA, Bandettini PA. Separating respiratory-variation-related fluctuations from neuronal-activity-related fluctuations in fMRI. Neuroimage. 2006 Jul; 31(4):1536–1548.

**Birn RM**, Murphy K, Handwerker DA, Bandettini PA. fMRI in the presence of task-correlated breathing variations. Neuroimage. 2009 Sep; 47(3):1092–1104.

**Bright MG**, Bulte DP, Jezzard P, Duyn JH. Characterization of regional heterogeneity in cerebrovascular reactivity dynamics using novel hypocapnia task and BOLD fMRI. Neuroimage. 2009; .

**Caballero-Gaudes C**, Reynolds RC. Methods for cleaning the BOLD fMRI signal. Neuroimage. 2017 Jul; 154:128–149.

**Cox RW**. AFNI: software for analysis and visualization of functional magnetic resonance neuroimages. Comput Biomed Res. 1996 Jun; 29(3):162–173.

**Dale AM**, Fischl B, Sereno MI. Cortical surface-based analysis. I. Segmentation and surface reconstruction. Neuroimage. 1999 Feb; 9(2):179–194.

**Esteban O**, Birman D, Schaer M, Koyejo OO, Poldrack RA, Gorgolewski KJ. MRIQC: Advancing the automatic prediction of image quality in MRI from unseen sites. PLoS One. 2017 Sep; 12(9):e0184661.

**Esteban O**, Blair R, Markiewicz CJ, Berleant SL, Moodie C, Ma F, Isik AI, Erramuzpe A, Kent JD, Goncalves M, DuPre E, Sitek KR, Poldrack RA, Gorgolewski KJ, poldracklab/fmriprep: 1.0.10; 2018.

**Fonov VS**, Evans AC, McKinstry RC, Almli CR, Collins DL. Unbiased nonlinear average age-appropriate brain templates from birth to adulthood. Neuroimage. 2009; 47:S102.

**Gorgolewski K**, Burns CD, Madison C, Clark D, Halchenko YO, Waskom ML, Ghosh SS. Nipype: a flexible, lightweight and extensible neuroimaging data processing framework in python. Front Neuroinform. 2011 Aug; 5:13.

**Gorgolewski KJ**, Esteban O, Ellis DG, Notter MP, Ziegler E, Johnson H, Hamalainen C, Yvernault B, Burns C, Manhães-Savio A, Jarecka D, Markiewicz CJ, Salo T, Clark D, Waskom M, Wong J, Modat M, Dewey BE, Clark MG, Dayan M, et al., Nipype: a flexible, lightweight and extensible neuroimaging data processing framework in Python. 0.13.1; 2017.

**Greve DN**, Fischl B. Accurate and robust brain image alignment using boundary-based registration. Neuroimage. 2009 Oct; 48(1):63–72.

**Huettel SA**, Song AW, McCarthy G, Others. Functional magnetic resonance imaging, vol. 1. Sinauer Associates Sunderland; 2004.

**Huijbers W**, Pennartz CMA, Beldzik E, Domagalik A, Vinck M, Hofman WF, Cabeza R, Daselaar SM. Respiration phase-locks to fast stimulus presentations: implications for the interpretation of posterior midline "deactivations". Hum Brain Mapp. 2014 Sep; 35(9):4932–4943.

**Jenkinson M**, Bannister P, Brady M, Smith S. Improved optimization for the robust and accurate linear registration and motion correction of brain images. Neuroimage. 2002 Oct; 17(2):825–841.

**Kastrup A**, Krüger G, Glover GH, Neumann-Haefelin T, Moseley ME. Regional variability of cerebral blood oxygenation response to hypercapnia. Neuroimage. 1999 Dec; 10(6):675–681.

**Kastrup A**, Li TQ, Glover GH, Moseley ME. Cerebral blood flow-related signal changes during breath-holding. AJNR Am J Neuroradiol. 1999 Aug; 20(7):1233–1238.

**Klein A**, Ghosh SS, Bao FS, Giard J, Häme Y, Stavsky E, Lee N, Rossa B, Reuter M, Chaibub Neto E, Keshavan A. Mindboggling morphometry of human brains. PLoS Comput Biol. 2017 Feb; 13(2):e1005350.

**Kundu P**, Brenowitz ND, Voon V, Worbe Y, Vértes PE, Inati SJ, Saad ZS, Bandettini PA, Bullmore ET. Integrated strategy for improving functional connectivity mapping using multiecho fMRI. Proc Natl Acad Sci U S A. 2013 Oct; 110(40):16187–16192.

**Napadow V**, Dhond R, Conti G, Makris N, Brown EN, Barbieri R. Brain correlates of autonomic modulation: combining heart rate variability with fMRI. Neuroimage. 2008 Aug; 42(1):169–177.

**Peirce JW**. Generating Stimuli for Neuroscience Using PsychoPy. Front Neuroinform. 2008; 2:10.

**Power JD**. A simple but useful way to assess fMRI scan qualities. Neuroimage. 2017 Jul; 154:150–158.

**Power JD**, Mitra A, Laumann TO, Snyder AZ, Schlaggar BL, Petersen SE. Methods to detect, characterize, and remove motion artifact in resting state fMRI. Neuroimage. 2014 Jan; 84:320–341.

**Power JD**, Plitt M, Gotts SJ, Kundu P, Voon V, Bandettini PA, Martin A. Ridding fMRI data of motion-related influences: Removal of signals with distinct spatial and physical bases in multiecho data. Proc Natl Acad Sci U S A. 2018 Feb; 115(9):E2105–E2114.

**Shmueli K**, van Gelderen P, de Zwart JA, Horovitz SG, Fukunaga M, Jansma JM, Duyn JH. Low-frequency fluctuations in the cardiac rate as a source of variance in the resting-state fMRI BOLD signal. Neuroimage. 2007 Nov; 38(2):306–320.

**Siegel JS**, Power JD, Dubis JW, Vogel AC, Church JA, Schlaggar BL, Petersen SE. Statistical improvements in functional magnetic resonance imaging analyses produced by censoring high-motion data points. Hum Brain Mapp. 2014 May; 35(5):1981–1996.

**Tustison NJ**, Avants BB, Cook PA, Zheng Y, Egan A, Yushkevich PA, Gee JC. N4ITK: improved N3 bias correction. IEEE Trans Med Imaging. 2010 Jun; 29(6):1310–1320.

**Winkler AM**, Ridgway GR, Webster MA, Smith SM, Nichols TE. Permutation inference for the general linear model. Neuroimage. 2014 May; 92:381–397.

**Wise RG**, Ide K, Poulin MJ, Tracey I. Resting fluctuations in arterial carbon dioxide induce significant low frequency variations in BOLD signal. Neuroimage. 2004 Apr; 21(4):1652–1664.

**Woolrich MW**, Ripley BD, Brady M, Smith SM. Temporal autocorrelation in univariate linear modeling of FMRI data. Neuroimage. 2001 Dec; 14(6):1370–1386.

**Zhang Y**, Brady M, Smith S. Segmentation of brain MR images through a hidden Markov random field model and the expectation-maximization algorithm. IEEE Trans Med Imaging. 2001 Jan; 20(1):45–57.